

Triadic Ca^{2+} Modulates Charge Movement in Skeletal Muscle

K STROFFKOVA* AND J A HEINY

*Department of Molecular and Cellular Physiology
University of Cincinnati College of Medicine
Cincinnati USA*

Abstract. The effects of intracellular Ca^{2+} changes on charge movement in frog skeletal muscle were investigated using high concentrations (10–20 mmol/l) of buffers with different abilities to buffer Ca^{2+} at distances close to the SR Ca^{2+} release channels. In BAPTA compared with EGTA perfused fibers charge movement was attenuated and lacked the characteristic kinetic features (I_3 and I_7) of E-C coupling charge movements. Q_{\max} decreased by 9 nC/ μF , V_{mid} was shifted 1.6 mV to more negative potentials and the steepness factor increased by 3.5 mV. Results of varying the holding potential suggested that BAPTA decreases the amount of charge available to move upon depolarization. Raising intracellular Ca^{2+} to micromolar levels at a fixed BAPTA concentration prevented the decline in Q_{\max} , suggesting that intracellular Ca^{2+} can modulate the amount of charge that is in the resting or available state. The different results obtained with BAPTA and EGTA can be explained by the greater ability of BAPTA to buffer dynamic Ca^{2+} changes at distances close to the release sites. These results are consistent with the proposals that an intracellular Ca^{2+} site on or near the dihydropyridine receptor, termed here the 'availability site', modulates the amount of charge available to move upon depolarization and is normally populated by Ca^{2+} released into the triad junction during activity.

Key words: Excitation-contraction coupling – Skeletal muscle – Charge movement

Correspondence to Dr J A Heiny, Department of Molecular and Cellular Physiology, University of Cincinnati, College of Medicine, Mail Box 67-0576, Cincinnati, OH 45267-0576, USA, Phone (513) 558-3115, Fax (513) 558-5738, E-mail heiny@ucbeh.edu

* Permanent address: Institute of Molecular Physiology and Genetics, Slovak Academy of Sciences, Vlarska 5, 83334 Bratislava, Slovakia

Introduction

Charge movement reflects conformational changes on the skeletal muscle dihydropyridine (DHP) receptor which controls the opening of Ca^{2+} release channels/ryanodine receptors on the sarcoplasmic reticulum (SR) during excitation-contraction coupling (E-C coupling). Ca^{2+} released into the triad junction diffuses to troponin where it binds to the activator sites for contraction.

High concentrations of the intracellular calcium buffer EGTA are commonly used to record charge movement in cut skeletal muscle fibers. EGTA buffers the Ca^{2+} that would normally reach troponin, thereby preventing contraction. Because of its slow ON rates, however, EGTA is not expected to buffer fast Ca^{2+} changes at distances closer to the release sites. Within the narrow gap between the transverse tubules and SR at the triadic junctions, Ca^{2+} levels may rise an order of magnitude greater than in the bulk myoplasm (Pizzagno et al. 1991). BAPTA, a calcium buffer derived from EGTA but with a faster ON rate, is a potentially more useful tool for manipulating dynamic Ca^{2+} changes at distances close to release sites (Tsien 1980). In skeletal muscle BAPTA is expected to buffer fast Ca^{2+} changes effectively to within 15–25 nm of the release channels (Neher 1986, Stern 1992, Anderson and Meissner 1995, Jong et al. 1996).

In this study we investigated the effects of intracellular Ca^{2+} on charge movement, using the different buffer kinetics of EGTA and BAPTA to separate the effects of triadic and myoplasmic Ca^{2+} changes. We found dramatic differences in charge movement that depended on whether EGTA or BAPTA was used to buffer intracellular Ca^{2+} . These results are explained by proposing that there is an intracellular Ca^{2+} site on the DHP receptor which can modulate the amount of charge available to move upon depolarization and is normally populated by Ca^{2+} released into the triadic space during activity.

Materials and Methods

Preparation

The experimental preparation protocols and recording apparatus were essentially the same as described previously (Henry and Jong 1990, Jong et al. 1997). Briefly, single cut skeletal muscle fibers from the semitendinosus muscle of *Rana catesbeiana* were voltage-clamped using the vaseline gap method. To improve the exchange of internal solution, the fiber segments in the end pools were treated briefly (1–2 mm) with a low concentration of saponin (0.01% in a Cs-glutamate internal solution). Thereafter the cut ends were rinsed thoroughly and perfused with a Cs-glutamate internal solution without saponin. This treatment also improves the quality of voltage clamp control by reducing voltage inhomogeneities under the vaseline seals (Gonzalez and Rios 1993). The holding potential was -90 mV, except

where indicated otherwise. Pulses were applied to the fiber and data was acquired using a microcomputer-based pulse generation and data acquisition system. The command pulse to the voltage clamp was low-pass filtered at a corner frequency of 3 kHz with an 8-pole Bessel filter. Membrane currents were filtered at 1.2 kHz using an 8-pole Bessel filter before being digitized.

Charge movement currents obtained using the standard holding potential (-90 mV) were elicited in response to test pulses of 200 ms duration superimposed on the holding potential. Linear leak and capacity currents were subtracted off-line using a small scaled control pulse applied from a subtracting holding potential of -110 mV. An alternate correction for linear leak and capacity was used for measurements of charge in depolarized fibers, as described in the legend to Fig. 4.

Solutions

The composition of the recording solutions is given in Table 1. The solutions were designed to eliminate all ionic currents. The osmolality of internal and external solutions was adjusted to 235 and 255 mOsm (± 5 mOsm), respectively. The pH was 7.1 at 8°C . The free Ca^{2+} concentration of the external solution was estimated as 1 mmol/l. The free Mg^{2+} concentration of the internal solutions was kept constant at 1 mmol/l. The internal solutions contained 10–20 mmol/l EGTA or BAPTA, yielding an estimated pCa_i of 9. pCa_i was raised for the experiments described in Table 4 by adding CaCl_2 to solution C. pCa_i and pMg_i values were estimated from published constants for the complexes of EGTA, BAPTA, CP, ATP, SO_4 and glutamate with protons, magnesium and calcium. An iterative program solved for the concentrations of the complexes using published equilibrium constants (Martell

Table 1. Solutions

Internal/end pools (mmol/l)										
Solution	C'sGlu	EGTA	BAPTA	MOPS	Na_2CP	Na_2ATP	MgSO_4	CaCl_2	glucose	pCa
A	70	20	0	10	5	5	6.48	0.078	5	9
B	50	0	20	10	5	5	6.83	0.039	5	9
C	66	0	10	10	5	5	6.38	0.019	5	9
External/central pool (mmol/l)										
Solution	TEA_2SO_4	CsSO_4	MOPS	CaSO_4	MgSO_4	CdSO_4	LnCl_3	$\text{TfTX}(\mu\text{mol/l})$		
D	85	5	5	3.25	0.5	0.5	0.1	1.56		

EGTA and MOPS were added as the free acid. BAPTA was added as the tetraacetium salt. The pH was adjusted using CsOH or TEA-OH.

and Smith 1974 Smith and Martell 1976 Godt and Lindley 1982) An equilibrium constant of 400 nanomolar was assumed for the CaBAPTA complex under physiological conditions (Harrison and Bers 1987) Constants for the complexes of BAPTA with protons were taken from Tsien (1980) Because BAPTA is largely tetravalent and EGTA is largely divalent at pH 7 the BAPTA containing internal solution is expected to have a higher ionic strength than the EGTA solution, for the same osmolarity The estimated ionic strengths of the BAPTA and EGTA internal solutions were 283 and 183 respectively Alternatively, for physiological measurements ionic equivalents may be the more relevant parameter (Godt and Maughan 1988) The ionic equivalence of the BAPTA and EGTA solutions were 160 and 145 respectively All experiments were performed at a temperature of $8 \pm 1^\circ\text{C}$

Initially we were not able to voltage clamp fibers for more than a few minutes after introducing BAPTA into the cut ends The BAPTA containing internal solution produced a large increase in holding current which was apparent as a sloping current baseline even on a single sweep We empirically found that adding 0.5 to 1.0 mmol/l Cd^{2+} to the external solution stabilized the holding current suggesting that BAPTA may have altered a Ca^{2+} -sensitive resting conductance or introduced a resting leak Fibers perfused with Cd^{2+} external solution and 10–20 mmol/l of intracellular BAPTA could be voltage-clamped for 1–2 hours

Protocol for introducing BAPTA into the myoplasm

BAPTA was introduced into the myoplasm through the cut ends However, based on the measured diffusion constant in frog myoplasm of the closely similar compound FURA 2 (Baylor and Hollingworth 1988) its diffusion is expected to be slow Assuming that BAPTA diffuses at a rate similar to FURA 2 we estimated the BAPTA concentration at the recording site using a model of one-dimensional diffusion down a cylinder for the boundary conditions of an extended initial distribution in the end pools (Crank 1975) Results are shown in Fig. 1 The main conclusion from this calculation was that the BAPTA concentration in the recording pool was not expected to reach equilibrium during our recording times Consequently we adopted a protocol in which diffusion was allowed to proceed at room temperature for 50–60 minutes after BAPTA solution was introduced into the cut ends At that time we cooled the fiber to 8°C voltage-clamped the fiber, and began recording Charge movement measurements were made during a time window of 60–80 minutes after the start of BAPTA diffusion (shaded region indicated in Fig. 1) The slow diffusion likewise precluded the washout of BAPTA and the comparison of EGTA and BAPTA effects in the same fiber Consequently whenever possible we used paired fibers dissected from the same muscle to compare charge movement in EGTA and BAPTA treated fibers

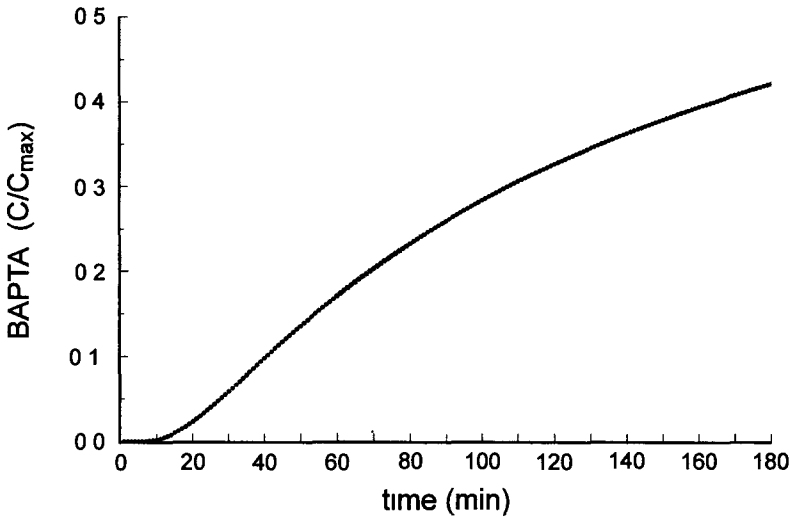


Figure 1. Estimated BAPTA concentration at the center of the recording pool at various times after BAPTA was applied to the end pools at a concentration C_{max} . The calculation assumes an apparent diffusion coefficient $0.4 \times 10^{-6} \text{ cm}^2/\text{s}$ taken from the apparent diffusion coefficient of FURA-2 in frog myoplasm at 16–17°C (Baylor and Hollingworth 1988). Shaded areas represent the time window during which charge movement was recorded, typically 60–80 minutes after the start of BAPTA perfusion. At this time, the expected BAPTA concentration in the central pool was 3.4–4.6 mmol/l for Solution B (20 mmol/l BAPTA) and 1.7–2.3 mmol/l for Solution C (10 mmol/l BAPTA).

Results

Dependence of charge movement properties on the identity of the intracellular calcium buffer: Differential effects of EGTA and BAPTA

Fig. 2 compares representative charge movement currents recorded in response to test depolarizations over the range -50 to 0 mV using either 20 mmol/l EGTA or 20 mmol/l BAPTA as the calcium buffer. Under these conditions, resting myoplasmic free Ca^{2+} is estimated to be $\sim 10^{-9}$ mol/l. With EGTA, charge movement currents display the characteristic kinetic features reported for skeletal muscle. The charge moved by a small voltage step to -50 mV shows a simple monotonic decay at the pulse ON and OFF. At depolarizations above -40 mV, the ON charge movement current has at least two kinetically distinct phases consisting of an early rapid decay and a delayed 'hump'. These features are similar to those reported by other laboratories for the Q_{β} and Q_{γ} components of charge movement (cf. review Rios and Pizarro 1991) which are most apparent in ON charge movement currents at voltages near threshold for Ca^{2+} release. At 0 mV, both components decayed

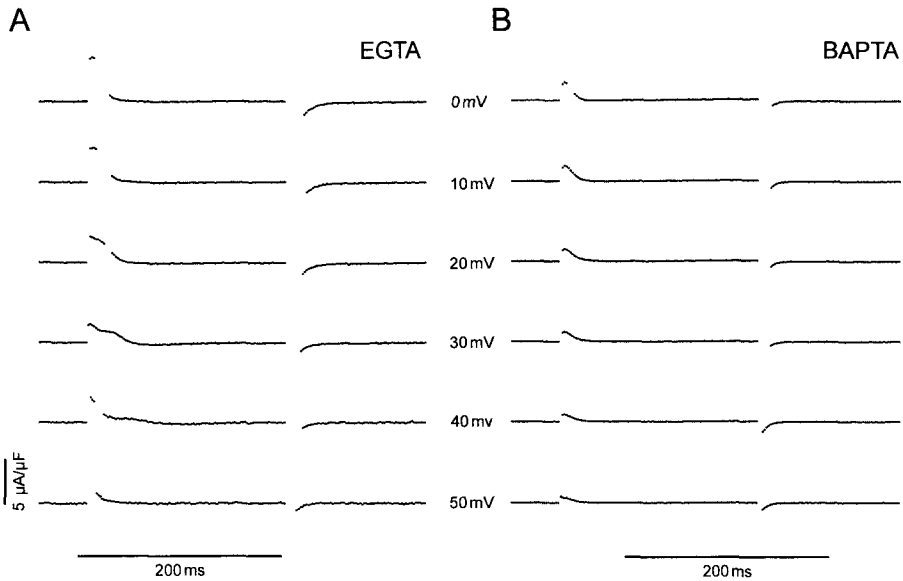


Figure 2. Charge movement currents recorded at the indicated test potential using either EGTA (A) or BAPTA (B) as the intracellular calcium buffer. Data were obtained from two fibers dissected from the same muscle and perfused with either 20 mmol/l EGTA (fiber reference 110692a) or 20 mmol/l BAPTA (fiber reference 110692b). Equilibrium fiber parameters are given in Table 2.

rapidly and merged together. OFF charge movement currents decayed monotonically upon returning to the holding potential from all test potentials. In contrast charge movement currents recorded with BAPTA were significantly attenuated and had no apparent I_T component at any voltage.

We next compared equilibrium charge movement parameters in EGTA and BAPTA solutions. Fig. 3A shows the charge voltage distribution obtained from the same fibers as in Fig. 2 perfused with either an EGTA (filled circles) or a BAPTA containing internal solution (open circles). In this experiment Q_{max} was significantly less in the BAPTA compared with the EGTA perfused fiber (12.5 nC/ μ F versus 28.0 nC/ μ F, respectively) and k was significantly greater (11.8 versus 6.1 mV, respectively). V_{mid} was not significantly different (-39.6 versus -38.7 mV, respectively). Fig. 3B displays the same data, normalized to illustrate the decreased steepness in BAPTA.

Table 2 summarizes the equilibrium charge movement parameters obtained from all fibers perfused with either EGTA (a) or BAPTA (b). Table 2c compares the differences in group means of the EGTA and BAPTA fibers. Table 2d compares the mean differences in these parameters when only paired fibers from the same muscle

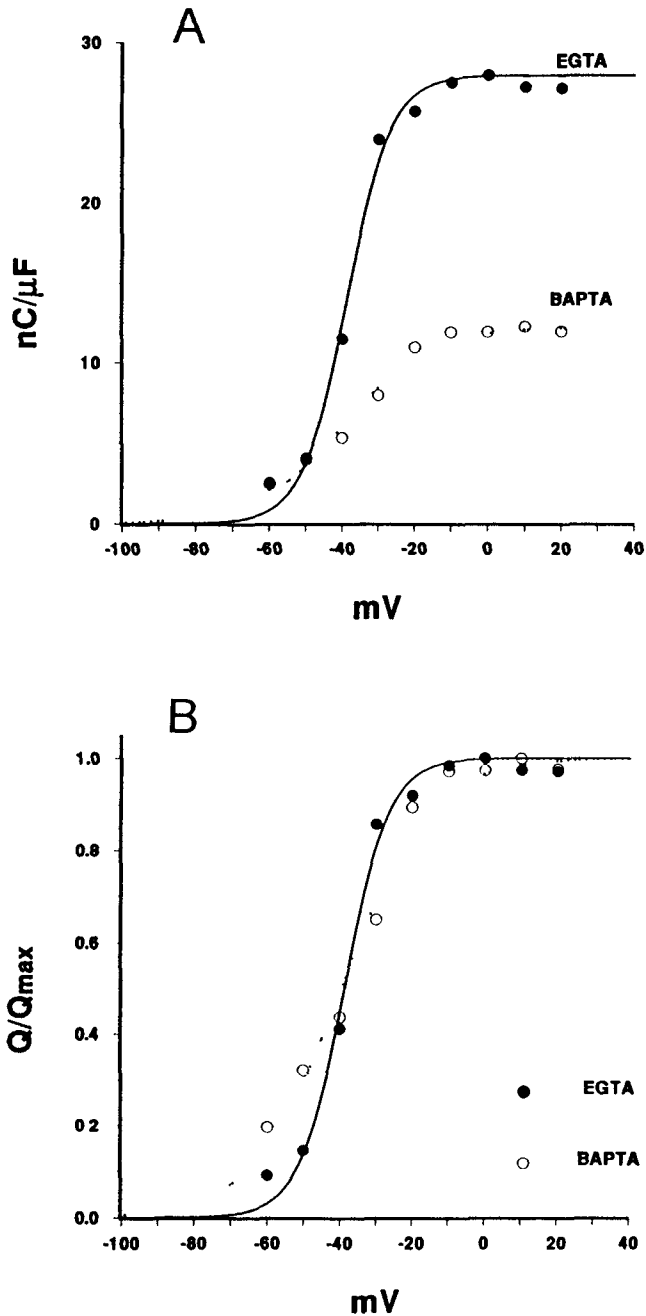


Figure 3. A) Equilibrium charge voltage distributions in EGTA (solid circles - continuous line) and BAPTA (open circles, dashed line) solutions, obtained from the same fibers as Fig. 2. The smooth lines are fitted values obtained using a two-state Boltzmann model. B) Same data normalized to maximum charge.

Table 2. Fiber parameters compared in EGTA and BAPTA containing internal solutions

a) 20 EGTA Internal					
Fiber Ref	C_m ($\mu\text{F}/\text{cm}^2$)	I_{Leak} ($\mu\text{A}/\mu\text{F}$)	Q_{max} ($\text{nC}/\mu\text{F}$)	V_{mid} (mV)	k (mV)
110692a	11.06	0.90	27.98	-38.69	6.09
111792a	10.01	1.03	30.66	-35.74	3.54
111992b	9.21	1.20	21.80	-28.21	5.11
102092a	8.06	1.03	26.60	-24.55	7.18
102092b	7.11	1.37	26.43	-21.90	10.32
102392a	8.07	0.94	31.13	-23.18	7.81
102792b	7.18	0.60	30.51	-25.83	11.69
102992a	9.72	0.86	29.81	-32.67	10.36
102992b	10.40	0.69	33.40	-34.67	5.06
Mean \pm S E M	9.0 ± 0.5	1.0 ± 0.1	28.7 ± 1.1	-29.5 ± 1.9	7.5 ± 0.9
b) 20 BAPTA Internal					
Fiber Ref	C_m ($\mu\text{F}/\text{cm}^2$)	I_{Leak} ($\mu\text{A}/\mu\text{F}$)	Q_{max} ($\text{nC}/\mu\text{F}$)	V_{mid} (mV)	k (mV)
110692b	11.03	1.56	12.49	-39.56	11.81
111792b	11.34	1.31	25.41	-35.69	8.74
111992a	9.50	1.49	15.34	-30.84	10.12
111192b	7.32	0.96	17.95	-38.04	8.73
110292a	11.13	1.04	19.26	-30.86	11.19
110392a	10.33	1.50	23.00	-39.92	9.41
110392b	8.33	1.50	23.51	-34.87	13.29
Mean \pm S E M	10.3 ± 0.8	1.3 ± 0.1	19.6 ± 1.8	-35.7 ± 1.4	10.5 ± 0.7
c) Differences in group means obtained from all fibers: grouped data for BAPTA ($n = 7$) and EGTA ($n = 9$)					
	ΔC_m ($\mu\text{F}/\text{cm}^2$)	ΔI_{Leak} ($\mu\text{A}/\mu\text{F}$)	ΔQ_{max} ($\text{nC}/\mu\text{F}$)	ΔV_{mid} (mV)	Δk (mV)
Mean	1.4	0.4	-9.1	-6.2	3.0
<i>P</i>	0.21	0.008	0.001	0.03	0.02
d) Mean differences in values from paired fibers (BAPTA - EGTA)					
	ΔC_m ($\mu\text{F}/\text{cm}^2$)	ΔI_{Leak} ($\mu\text{A}/\mu\text{F}$)	ΔQ_{max} ($\text{nC}/\mu\text{F}$)	ΔV_{mid} (mV)	Δk (mV)
Mean \pm S E M ($n = 3$)	0.53 ± 0.24	0.4 ± 0.1	-9.1 ± 1.9	-1.1 ± 0.5	5.3 ± 0.1
<i>P</i>	0.33	0.08	0.11	0.28	0.002

were included. On average Q_{\max} was reduced by 9 nC/ μF in BAPTA compared with EGTA perfused fibers, V_{mid} was shifted 1.6 mV to more negative potentials and the steepness factor increased by 3.5 mV. We consider the paired group to be the most reliable data, since we have observed in general that charge movement parameters are more similar in fibers from the same muscle than from different muscles. However, the significance was less in the paired group, as expected from the greater variance with a small sample. These effects could not be attributed to changes in linear fiber parameters. Membrane capacity (C_m) was similar in the EGTA and BAPTA solutions but there was a tendency for fibers in BAPTA to develop more leak, assessed as the steady current (I_{leak}) measured at the end of a pulse to -120 mV from the holding potential. I_{leak} was 40% greater in the BAPTA than in the EGTA solution. Changes in I_{leak} could have resulted from changes in a sarcolemmal or T-system resting conductance or seal leak. The fact that the increase in I_{leak} was not accompanied by a change in membrane capacitance implies that the amplitude of the voltage change in the T-system which is the immediate driving force for charge movement, was not significantly different in the two solutions (Ashcroft et al. 1985).

Effect of holding potential on the charge measured in BAPTA perfused fibers

The finding that the kinetics and voltage-dependence of charge movement differed depending on whether EGTA or BAPTA was used to buffer calcium was not expected since the buffers have approximately the same equilibrium capacity and affinity for Ca^{2+} . This discrepancy prompted us to investigate the basis for these differences.

In BAPTA less charge moved upon depolarization in the voltage range positive to the holding potential. The charge that remained moved with a less steep voltage-dependence and without the characteristic kinetic features (Q_β and Q_γ) that define E-C coupling charge movements. These features are similar to those of fibers subjected to prolonged depolarization which causes the disappearance of charge that moves over the voltage range -90 to 0 mV (Charge 1) and the appearance of a charge (Charge 2) that moves over a more negative voltage range with a significantly broader voltage-dependence (Adrian and Almers 1976; Chandler et al. 1976). Charge 2 may reflect an inactivated conformation of the DHP receptor resulting from a voltage-modulated state change (Brum and Rios 1987), or alternatively it may be a separate species of charge (Huang 1993).

We therefore considered the possibility that BAPTA might produce an effect on charge movement similar to sustained depolarization—that is, it might reduce the charge that is available to move upon depolarization and increase the charge that moves at more negative voltages. To test this we measured charge movement in both polarized (holding potential -120 mV) and depolarized fibers (holding potential = 0 mV), in 10 mmol/l BAPTA. The results are shown in Fig. 4A.

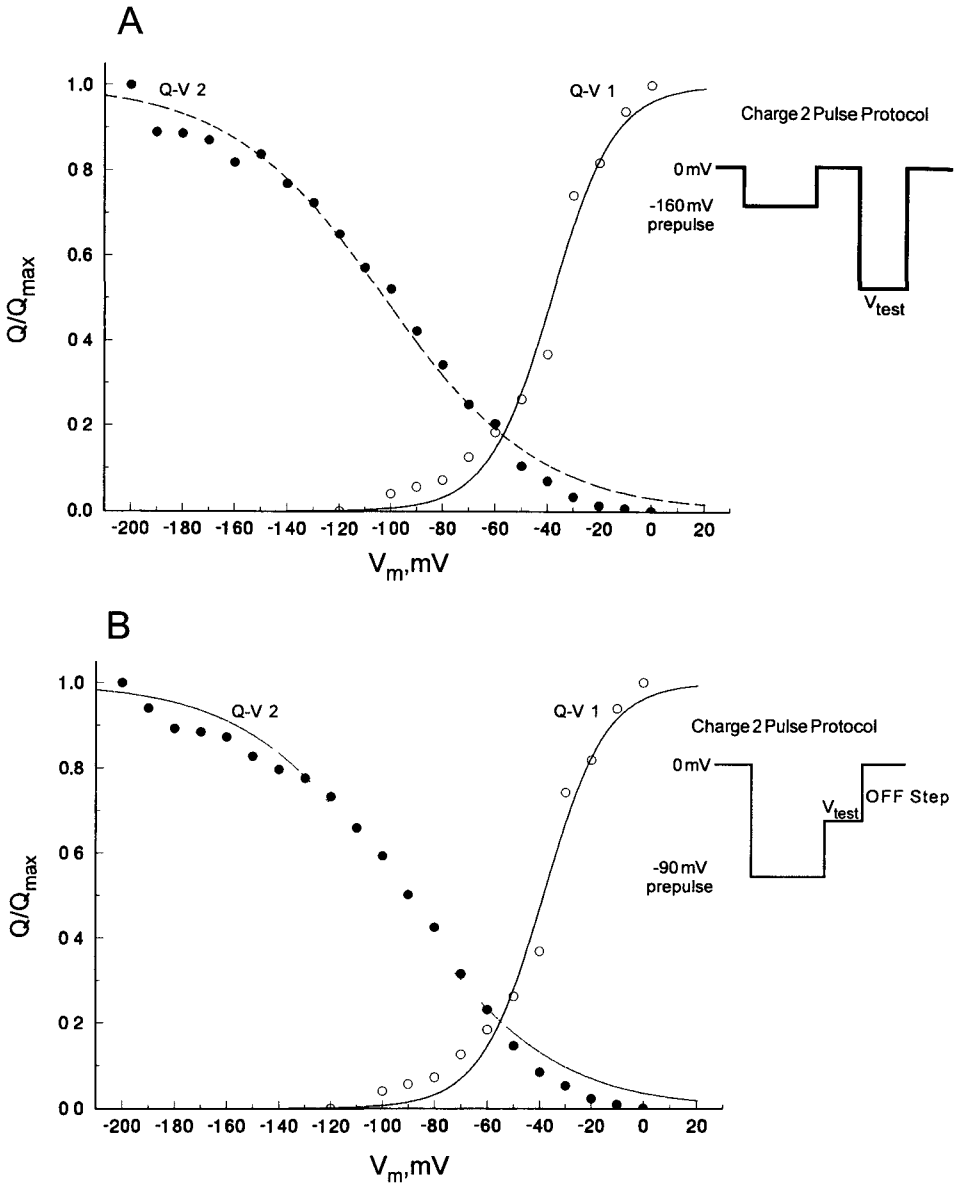


Figure 4. Effect of holding potential on charge movement in fibers perfused internally with 10 mmol/l BAPTA. The charge-voltage distributions were obtained using a holding potential of -120 mV ($Q-V 1$, \circ) or 0 mV ($Q-V 2$, \bullet). **A**) Charge moving from the depolarized holding potential was recorded using the pulse protocol shown (inset) in which the test pulse was preceded by a hyperpolarizing conditioning pulse to minimize ionic currents flowing in this voltage range (Brum and Rios 1987). A positive going control

Hyperpolarizing the fiber to -120 mV ($Q-V$ 1, open circles) is expected to recruit all of the charge available to move upon depolarization (Charge 1). In this fiber, Q_{\max} was 33.6 nC/ μF , V_{mid} was -38.6 mV and $k = 12.0$ mV. The mean values for three similar measurements are given in Table 3, row 1. On average, Q_{\max} was 63% greater in the hyperpolarized, BAPTA perfused fibers than in fibers held at -90 mV (Table 2b). V_{mid} and k were within the range of values measured from the -90 mV holding potential. Thus it appears that membrane potential can reverse some of the reduction in Charge 1 that was observed with BAPTA at the normal -90 mV holding potential, making additional charge available to move upon depolarization. On the other hand, when fibers were held at 0 mV ($Q-V$ 2, closed circles), more charge moved than in polarized fibers and it had a less steep voltage-dependence, resulting in a broad charge distribution extending from -180 up to 0 mV.

A similar result was obtained when this measurement was repeated using an alternative pulse protocol (Szucs et al. 1991), as shown in Fig. 4B. Table 3 summarizes the effect of holding potential on the distribution of charge measured from either a polarized or depolarized holding potential. Q_{\max} in polarized fibers was increased further by hyperpolarization (-120 mV compared with -90 mV HP). Additionally, irrespective of the method used to measure Charge 2, Q_{\max} in depolarized fibers was larger than in polarized fibers held at -120 mV, its midpoint was shifted to more negative potentials and k increased. Thus, the voltage dependence of the charge that moves in depolarized fibers is such that it would alter the charge measured from the standard -90 mV holding potential if it were present in normally polarized fibers (Hui and Chandler 1990). If BAPTA increased this charge, the net result would be that the measured Charge 1 would be reduced, shifted to more negative voltages and have a smaller apparent valence. Taken together, these results are consistent with the idea that BAPTA may be doing something equivalent to sustained depolarization—that is, it may promote the movement of charge into an unavailable or inactive state. The fact that hyperpolarization can reverse some of the reduction in charge produced by BAPTA indicates that BAPTA

pulse (0 to $+30$ mV) was used for both polarized and depolarized holding potentials to avoid contributions to the control pulse from Charge 2 moving near the normal -90 mV holding potential. This is expected to minimize any possible residual charge moving in control pulses. Additionally, the use of saponin in the cut ends effectively eliminates voltage inhomogeneities under the vaseline seals, reducing changes in steepness due to charge moving in these regions (Hui and Chandler 1990; Gonzalez and Rios 1993). The smooth lines represent a fit of each data set to a single Boltzmann function. Fitted parameters for $Q-V$ 1 were $Q_{\max} = 33.6$ nC/ μF , $V_{\text{mid}} = -38.6$ mV, $k = 12.1$ mV. Parameters for $Q-V$ 2 were $Q_{\max} = 12.7$ nC/ μF , $V_{\text{mid}} = -102.6$ mV, $k = 29.6$ mV. B) Same experiment repeated using an alternate protocol (inset) in which inactivated charge was measured using the 'stepped OFF' protocol of Szucs et al. (1991). In this case fitted parameters for $Q-V$ 2 were $Q_{\max} = 39.6$ nC/ μF , $V_{\text{mid}} = -94.0$ mV, $k = 28.5$ mV.

Table 3 Mean $Q - V$ parameters in polarized and depolarized fibers perfused with BAPTA

HP (mV)	Pulse Protocol	N	Q_{max} (nC/ μ F)	V_{mid} (mV)	k (mV)
-120	simple step	3	33.82 ± 1.15	-10.24 ± 0.50	13.33 ± 0.39
0	conditioning prepulse	3	47.81 ± 1.53	-102.76 ± 0.25	27.28 ± 0.94
0	stepped OFF	3	45.66 ± 1.76	-89.66 ± 1.85	27.63 ± 0.15

Charge 1 was determined using a simple step from the holding potential (HP). Charge 2 was determined using either a conditioning prepulse (Bium and Rios 1987) or a stepped OFF protocol (Szucs et al. 1991). In all cases, the control pulse was a step to +30 mV from 0 mV.

has not eliminated charge, but rather altered its distribution among available and unavailable states.

Effect of intracellular resting $[Ca^{2+}]$ on the charge measured in BAPTA perfused fibers

We next addressed the question of whether the effects of BAPTA were due to its Ca^{2+} buffering action or some indirect effect. In the experiments described above, BAPTA was used at $pCa_i \sim 9$ following the standard protocol in the cut fiber preparation for blocking contraction. In the next series of experiments, charge movement was compared at different intracellular free Ca^{2+} concentrations selected to test three limiting cases. These were $pCa_i = 9$ (the standard resting pCa_i for charge movement measurements), $pCa_i = 7$ (near the physiological resting Ca^{2+} level) and $pCa_i = 6.5$ which is the just sub-threshold concentration for eliciting contraction. The measurements were made using a HP of -120 mV to remove any additional effects of voltage on the $Q - V$ distribution. The results are shown in Table 4. Increasing intracellular free Ca^{2+} from $pCa_i 9$ to $pCa_i 6.5$ significantly increased Q_{max} , preventing the BAPTA induced decrease.

The finding that Q_{max} varies with pCa_i for the same BAPTA concentration indicates that the effects of BAPTA on charge movement occur via its Ca^{2+} buffering actions, and not via some indirect or pharmacologic mechanism. This result also indicates that the amount of charge available to move upon depolarization can be modulated by intracellular Ca^{2+} . The complete Q_{max} versus pCa_i relationship cannot be measured in an isolated fiber. Nevertheless, the steepest increase in Q_{max} occurred over the range $pCa_i 7$ to $pCa_i 6.5$ (Table 4), suggesting that BAPTA is buffering intracellular Ca^{2+} at a site with an affinity for Ca^{2+} in the micromolar or higher range. This is an order of magnitude above normal resting myoplasmic Ca^{2+} levels (about 0.1 μ mol/l) indicating that only activity-related Ca^{2+} changes could populate this site. The overall conclusion from these measurements is that

Table 4. Effects of varying intracellular Ca^{2+} on the $Q - V$ distribution from polarized fibers (holding potential = -120 mV) perfused with BAPTA

Ca_o mmol/l	Ca_i pCa	Q_{\max} nC/ μF	V_{mid} mV	k mV
1	9	33.82 ± 1.15	-40.24 ± 0.50	13.33 ± 0.39
1	7	38.88 ± 1.26	-41.49 ± 1.07	15.47 ± 0.28
1	6.5	52.41 ± 0.88	-40.86 ± 0.33	15.38 ± 0.75
1	6*			

*Fiber contracted in pCa = 6, confirming the validity of the estimated L_d for BAPTA in frog myoplasm

BAPTA reduces Q_{\max} by buffering a pool of free Ca^{2+} that normally reaches supra-micromolar levels and populates an intracellular Ca^{2+} site that controls the amount of available charge

Source of the modulator Ca^{2+}

The finding that intracellular Ca^{2+} can modulate the amount of available charge does not in itself explain the different results obtained with BAPTA and EGTA. Both EGTA and BAPTA are expected to buffer resting pCa_i to the nmol/l range at equilibrium. This prompted us to ask: what intracellular Ca^{2+} pool reaches micromolar levels and would be buffered differentially by BAPTA and EGTA? We postulated that this could be the triadic space where intracellular Ca^{2+} reaches supra-micromolar concentrations during Ca^{2+} release from the SR; additionally, the ability of BAPTA and EGTA to buffer dynamic Ca^{2+} changes can be very different from their equilibrium buffering properties. These differences result from their different ON rates and are expected to be greatest at distances close to the release sites (Neher 1986; Stein 1992; Jong et al. 1996). Therefore we estimated the free Ca^{2+} concentration at distances close to the release sites under our experimental conditions. The results are shown in Fig. 5.

This calculation shows that during Ca^{2+} release, BAPTA but not EGTA is expected to effectively buffer Ca^{2+} changes near the release sites. Both buffers would effectively buffer myoplasmic Ca^{2+} changes at distances $> 100 - 200$ nm from the release sites. In other words, with BAPTA both triadic and myoplasmic Ca^{2+} changes will be buffered; with EGTA, a compartmentalization of free Ca^{2+} is established whereby myoplasmic Ca^{2+} changes are buffered while triadic Ca^{2+} changes go on essentially unperturbed. The conclusion from this calculation is that the modulator Ca^{2+} which BAPTA is buffering is a local transient Ca^{2+} pool located within nm of the release sites, i.e. within the triadic space.

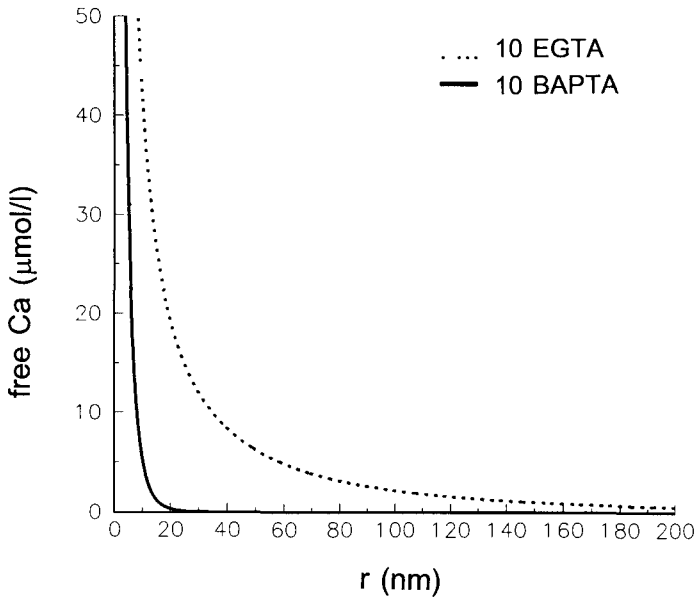


Figure 5. Expected free Ca^{2+} changes during activity at different distances r (nm) from the release sites when Ca^{2+} buffers are present in the bulk solution. Based on model of Stern (1992) using the constants: apparent $D_{\text{Ca}} = 3 \times 10^{-6} \text{ cm}^2/\text{s}$, $[\text{EGTA}]_0 = 10 \text{ mmol/l}$, $[\text{BAPTA}]_0 = 10 \text{ mmol/l}$, k_{on} for EGTA = $2.5 \times 10^6 \text{ mol}^{-1} \text{ s}^{-1}$, k_{on} for BAPTA = $1.7 \times 10^7 \text{ mol}^{-1} \text{ s}^{-1}$, K_d for EGTA = 158 nmol/l , K_d for BAPTA = 100 nmol/l , flux through Ca release channel = 10^4 ions/s , l_{Ca} , the characteristic diffusion length for a Ca^{2+} ion was 140 nm in the EGTA solution and 5 nm in the BAPTA solution.

Discussion

Major findings

The main finding of this study is that intracellular Ca^{2+} can modulate the amount of charge available to move upon depolarization. The charge moved by depolarization represents the charge available to do $E-C$ coupling. The greater effectiveness of BAPTA in buffering this Ca^{2+} indicates that the modulator pool is located near the release channels of the SR, within the junctional gap. The K_d of the site, estimated to be at least an order of magnitude above the resting myoplasmic Ca^{2+} concentration, indicates that it would normally be populated only during activity by Ca^{2+} released from the SR. These results are consistent with the proposals that a Ca^{2+} site on an internal domain of the DHP receptor can modulate the amount of charge in the resting or available state, and that this site is populated by Ca^{2+} ions released into the triadic space during activity. We refer to it as the 'availability site'.

In cut skeletal muscle fibers perfused with EGTA, this site is not populated at rest but is expected to become populated upon depolarization when triadic Ca^{2+} exceeds micromolar concentrations and is essentially unperturbed by the buffer. Consequently, more charge becomes available to move with the next depolarization. In BAPTA perfused fibers, this site is not populated either at rest or during activity because of the greater effectiveness of BAPTA as a Ca^{2+} buffer near the release sites. Thus, the initial distribution of charge does not change with depolarization. We expect that intact fibers may represent an intermediate situation. Without added calcium buffers, their higher resting pCa_i favors more charge initially in the available state, and a smaller redistribution upon depolarization.

Mechanism of action and molecular identity of the 'availability site'

Released Ca^{2+} could alter DHP receptor conformation directly by binding to an internal domain, or indirectly, for example by activating a Ca^{2+} dependent enzyme which modifies the channel. Molecular studies have identified several putative Ca^{2+} sites on internal domains of the DHP receptor (Tanabe et al 1987). However to date no functional correlates have been demonstrated for them. Similarly, putative phosphorylation sites have been identified which could be substrates for a Ca^{2+} -dependent kinase or phosphatase (Jahn et al 1988, Chang et al 1991, Ma et al 1992).

Independent functional studies have identified several Ca^{2+} sites on the DHP receptor which are important for modulating the distribution of charge in the available state. However none of these sites appears to match the profile of the 'availability site' revealed by this study. Rios et al (1990) characterized a Ca^{2+} site termed the 'priming site' which is accessible from the extracellular space and whose affinity is modulated by membrane potential. Ca^{2+} bound to the site maintains charge in the resting or available state but dissociates upon depolarization, thereby converting charge into inactive states. Schmier et al (1993) estimated the dissociation constants for Ca^{2+} from this site to be $< 5 \times 10^{-8}$ molar in the resting conformation, and > 35 millimolar for the active state. It is likely that the 'availability site' suggested by our results is distinct from the 'priming site' since intracellularly applied BAPTA should not have access to the latter. Moreover, under our conditions of extracellular Ca^{2+} , Ln^{3+} & Cd^{2+} , the DHP receptor is expected to be highly stabilized in the available state at the 'priming site'. Thus, our results suggest that at least two Ca^{2+} sites may control whether the DHP receptor is available to move upon depolarization. It is possible that more than one transition may lead to the available state - one controlled by the external 'priming site' and one by the internal 'availability site'. The internal Ca^{2+} site identified in our study may control a transition from an unavailable (but not necessarily inactive) state to the available state.

Rios and collaborators have also proposed the existence of internal low affinity

($K_d \sim 16\text{--}20 \mu\text{mol/l}$ Pizzano et al 1991, $10 \mu\text{mol/l}$ Shirokova et al 1994) Ca^{2+} -sites termed the ' γ sites', which bind released Ca^{2+} on or near the DHP receptor and increase the local surface potential. The added depolarization causes more charge to move, generating additional Q_γ charge movement in a positive feedback manner. Thus the γ -sites promote the transition from the resting or available state to the active E-C coupling conformation. In comparison, the availability site controls a different transition from unavailable to the resting or available state and can modulate the amount of initial charge available to undergo the depolarization dependent transition. Based on this profile, the availability site revealed in this study appears to be separate from the ' γ -sites' unless the same site can modulate both transitions.

Some recent studies of Ca^{2+} channel currents in skeletal muscle may be relevant to the availability site for charge movement. Feldmeyer et al (1993) showed that the Ca^{2+} current gradually declined and eventually was completely inhibited in frog fibers perfused with intracellular BAPTA or ruthenium red, a blocker of SR Ca^{2+} release. They concluded that Ca^{2+} release from the SR regulates the skeletal muscle L-type Ca^{2+} channel, and speculated that binding of Ca^{2+} to an internal site may be important for maintaining channel activity. Charge movement was not measured in that study but a decline in Ca^{2+} current is consistent with a reduced number of channels in the available state.

Recently Fleig and Penner (1995, 1996) report that a subset of silent Ca^{2+} channels become primed by strong and long lasting depolarizations to conduct Ca^{2+} current upon repolarization, generating excessive tail currents. They attribute this to a direct interaction between the DHP sensitive Ca^{2+} channel and ryanodine receptor during depolarization and speculate that a similar mechanism may underlie the phenomenon of voltage dependent facilitation of the Ca^{2+} current (Sculptoreanu et al 1993, Fleig and Penner 1996). This mechanism in which the ryanodine receptor not released Ca^{2+} ions, interacts with and 'primes' the Ca^{2+} channel likewise differs from the availability site mechanism postulated here.

In summary molecular and functional studies have identified a number of putative Ca^{2+} sites on the DHP receptor/skeletal Ca^{2+} channel. Results of this work support data from other studies that suggest that the state of the channel and/or the number of activatable Ca^{2+} channels is influenced by local, dynamic Ca^{2+} changes in the junctional gap in a depolarization dependent manner. Clearly more studies are needed to integrate data from charge movement and calcium current measurements, and to identify the underlying structure-function relationships at the molecular level.

Acknowledgements. This work was supported by the National Institute of Arthritis and Musculoskeletal and Skin Diseases of the National Institutes of Health U.S.A. (RO1 AR40213) and by the American Heart Association (Established Investigator Award to J. A. H.).

References

- Adrian R H, Almers W (1976) The voltage dependence of membrane capacity *J Physiol (London)* **254**, 317–338
- Anderson K, Meissner G (1995) T-tubule depolarization induced SR Ca^{2+} release is controlled by dihydropyridine receptor- and Ca^{2+} -dependent mechanisms in cell homogenates from rabbit skeletal muscle *J Gen Physiol* **105**, 363–383
- Ashcroft F M, Hemy J A, Vergara J (1985) Inward rectification in the T-system of frog skeletal muscle studied with potentiometric dyes *J Physiol (London)* **359**, 269–291
- Baylor S M, Hollingworth S (1988) FURA-2 Calcium transients in frog skeletal muscle fibres *J Physiol (London)* **403**, 151–192
- Brum G, Rios E (1987) Intramembrane charge movement in skeletal muscle fibres. Properties of Charge 2 *J Physiol (London)* **387**, 489–517
- Chandler W K, Rakowski R F, Schneider M F (1976) Effects of glycerol treatment and maintained depolarization on charge movement in skeletal muscle *J Physiol (London)* **254**, 285–316
- Chang C F, Gutierrez L M, Mundina Weilenmann C, Hosey M M (1991) Dihydropyridine sensitive calcium channels from skeletal muscle. 2. Functional effects of differential phosphorylation of channel subunits *J Biol Chem* **266**, 16395–16400
- Crank J (1975) *The Mathematics of Diffusion*. Clarendon Press, Oxford
- Feldmeyer D, Melzer W, Pohl B, Zollner P (1993) A possible role of sarcoplasmic Ca^{2+} release in modulating the slow Ca^{2+} current of skeletal muscle. *Pflug Archiv Eur J Physiol* **425**, 54–61
- Fleig A, Penner R (1995) Excessive repolarization dependent calcium currents induced by strong depolarizations in rat skeletal myoballs. *J Physiol (London)* **489**, 41–53
- Fleig A, Penner R (1996) Silent calcium channels generate excessive tail currents and facilitation of Ca^{2+} currents in rat skeletal myoballs. *Biophys J* **70**, A186
- Godt R E, Lindley B D (1982) Influence of temperature upon contractile activation and isometric force production in mechanically skinned muscle fibers of the frog. *J Gen Physiol* **80**, 279–297
- Godt R E, Maughan D W (1988) On the composition of the cytosol of relaxed skeletal muscle of the frog. *Amer J Physiol* **254**, C591–C604
- Gonzalez A, Rios E (1993) Perchlorate enhances transmission in skeletal muscle: excitation-contraction coupling. *J Gen Physiol* **102**, 373–421
- Harrison S M, Bers D M (1987) The effect of temperature and ionic strength on the apparent Ca -affinity of EGTA and the analogous Ca -chelators BAPTA and dibromo-BAPTA. *Biochim Biophys Acta* **925**, 133–143
- Hemy J A, Jong D (1990) A nonlinear electrostatic potential change from the T system of skeletal muscle detected under passive recording conditions using potentiometric dyes. *J Gen Physiol* **95**, 147–175
- Huang C L (1993) Charge inactivation in the membrane of intact frog striated muscle fibres. *J Physiol (London)* **468**, 107–124
- Hui C S, Chandler W K (1990) Intramembraneous charge movement in frog cut twitch fibers mounted in a double vaseline-gap chamber. *J Gen Physiol* **96**, 257–297

- Jahn H, Nastanczyk W, Rohrkasten A, Schneider T (1988) Site-specific phosphorylation of the purified receptor for calcium-channel blockers by cAMP- and cGMP-dependent protein kinases, protein kinase C, calmodulin-dependent protein kinase II and casein kinase II *Eur J Biochem* **178**, 535–542
- Jong D, Pape P C, Giebel J and Chandler W K (1996) Sarcoplasmic reticulum calcium release in frog cut muscle fibers in the presence of a large concentration of EGTA. In *Organellar Ion Channels and Transporters* 19th Annual Symposium of the Society of General Physiologists (Eds D E Clapham B E Ehrlich) pp 256–268 Rockefeller University Press
- Jong D S, Stroffekova K, Heiny J A (1997) A surface potential change in the membranes of frog skeletal muscle is associated with excitation-contraction coupling. *J Physiol (London)* **499**, 787–808
- Ma J, Gutierrez L M, Hosey M M, Rios E (1992) Dihydropyridine-sensitive skeletal muscle Ca channels in polarized planar bilayers. 3 Effects of phosphorylation by protein kinase C *Biophys J* **63**, 639–647
- Martell A E, Smith R M (1974) *Critical Stability Constants* Vol 1 Plenum Press New York
- Neher E (1986) Concentration profiles of intracellular calcium in the presence of a diffusible chelator. In *Calcium Electrogenesis and Neuronal Functioning* (Eds U Heinemann M Klee E Neher and W Singer) pp 80–96, Springer-Verlag Berlin and Heidelberg
- Pizarro G, Csernoch L, Uribe I, Rodriguez M, Rios E (1991) The relationship between Q_7 and Ca release from the sarcoplasmic reticulum in skeletal muscle. *J Gen Physiol* **97**, 913–947
- Rios E, Fitts R, Uribe I, Pizarro G, Brum G (1990) A third role for calcium in excitation-contraction coupling. In *Transduction in Biological Systems* (Eds C Hidalgo et al) pp 385–399 Plenum Press New York
- Rios E, Pizarro G (1991) Voltage sensor of excitation-contraction coupling in skeletal muscle. *Physiol Rev* **71**, 849–908
- Schmer A, Luttgau H C, Melzer W (1993) Role of extracellular metal cations in the potential dependence of force inactivation in skeletal muscle fibres. *J Muscle Res Cell Motil* **14**, 565–572
- Sculptoreanu A, Scheuer T, Catterall W A (1993) Voltage-dependent potentiation of L-type Ca^{2+} channels due to phosphorylation by cAMP-dependent protein kinase. *Nature* **364**, 240–243
- Shuokova N, Pizarro G, Rios E (1994) A damped oscillation in the intramembraneous charge movement and calcium release flux of frog skeletal muscle fibers. *J Gen Physiol* **104**, 449–476
- Smith R M, Martell A E (1976) *Critical Stability Constants* Vol 4 Inorganic Complexes Plenum Press New York
- Stern M D (1992) Buffering of calcium in the vicinity of a channel pore. *Cell Calcium* **13**, 183–192
- Szucs G, Papp Z, Csernoch L, Kovacs L (1991) Kinetic properties of intramembraneous charge movement under depolarized conditions in frog skeletal muscle fibers. *J Gen Physiol* **98**, 365–378
- Tanabe T, Takeshima H, Mikami A, Flockerzi V, Takahashi H, Kangawa K, Kojima M, Matsuo H, Hirose T, Numa S (1987) Primary structure of the receptor for calcium channel blockers from skeletal muscle. *Nature* **328**, 313–318

Tsien R. Y. (1980) New calcium indicators and buffers with high selectivity against magnesium and protons: design, synthesis and properties of prototype structures
Biochemistry USA **19**, 2396—2404

Final version accepted March 29, 1997